AXIALLY SYMMETRIC FOCUSING OF LIGHT IN DRY LASER CLEANING AND NANOPATTERNING

J. KOFLER AND N. ARNOLD

Institute for Applied Physics, Johannes Kepler University Linz, Altenbergerstrasse 69, 4040 Linz, Austria
johannes.kofler@jku.at and nikita.arnold@jku.at

The field enhancement by spherical particles plays a fundamental role in nanopatterning and in dry laser cleaning where such particles are used as model contaminants. We describe the general vectorial axially symmetric and strongly aberrated focusing by matching the solution of geometrical optics with a wave field built by the integral canonical for this topology, i.e., the Bessoid integral. For the focusing by transparent spheres with a few wavelengths in diameter, the results are much more compact and intuitive than the Mie theory. The results of the latter are reproduced with good agreement down to Mie parameters of about 30. Analytical expressions for the intensity on the axis and the position of the diffraction focus are derived.

1. Introduction

In this work we describe theoretically the focusing of light by transparent spheres with diameters of several wavelengths. Such focusing plays an important role in dry laser cleaning [1, 2] and has been used lately for different types of high-throughput laser material processing [3].

Strong spherical aberration makes the focusing non-trivial. Usually, the exact solution is obtained using the Mie theory [4], which does not give much of a physical insight as it is based on a multipole expansion. At the same time, the main focusing properties of transparent dielectric spheres originate rather from the picture of geometrical optics.

In the lowest approximation the sphere acts as an ideal lens. In many cases this picture does not even provide a description which is qualitatively correct. Also classical formulas for *weak* spherical aberration [5] do not yield useful results for the field behind a sphere: The maximum intensity is kept unchanged and its position does not depend on the wavelength.

Our approach — following the method of uniform caustic asymptotics in Ref. [6] — is based on the canonical integral for the cuspoid ray topology of

strong spherical aberration. Though this Bessoid integral appears naturally in small angles approximation, it can be used to describe *arbitrary* axially symmetric strong spherical aberration by appropriate coordinate and amplitude transformations. For angularly dependent vectorial amplitudes the formalism uses higher-order Bessoid integrals.

The Bessoid integral is the axially symmetric generalization of the Pearcey integral [7], which plays an important role in many short wavelength phenomena [8].

2. The Bessoid Integral

2.1. *Definition*

We first consider the diffraction of a *scalar* spherically aberrated wave on a circular aperture with radius a in the plane $z = -f$ around the z-axis, where f is the focal distance. The origin of the coordinate system is put into the focus F. In cylindrical coordinates (ρ, z) and small angle approximation, the Fresnel–Kirchhoff diffraction integral [5] yields the field amplitude

$$U(\rho, z) = -\frac{\mathrm{i}\, k\, U_0}{f}\, \mathrm{e}^{\,\mathrm{i}\, k\, z} \int_0^a J_0\!\left(k\, \frac{\rho\, \widetilde{\rho}_1}{f}\right) \mathrm{e}^{-\mathrm{i}\, k\, \frac{z\, \widetilde{\rho}_1^2}{2\, f^2} - \mathrm{i}\, k\, B\, \widetilde{\rho}_1^4}\, \widetilde{\rho}_1\, \mathrm{d}\widetilde{\rho}_1. \qquad (1)$$

Here U_0 is the amplitude of the incident wave in the center of the aperture, k is the wavenumber ($k = 2\pi/\lambda$, where λ is the wavelength) and $\widetilde{\rho}_1$ is the distance from the axis on the aperture. The Bessel function J_0 comes from the integration over the polar angle φ. The parameter B in the exponent determines the strength of the spherical aberration. For $B > 0$ the diffraction focus shifts towards the aperture, while $B = 0$ corresponds to ideal focusing [5].

We introduce dimensionless coordinates $\rho_1 \equiv \sqrt[4]{4\, k\, B}\, \widetilde{\rho}_1$, $R \equiv \sqrt[4]{k^3/4\, B}\, \rho/f$ and $Z \equiv \sqrt{k/4\, B}\, z/f^2$ and consider an infinitely large aperture. Then the field (1) becomes proportional to the *Bessoid integral* [9]

$$\begin{aligned} I(R, Z) &= \int_0^\infty \rho_1\, J_0(R\, \rho_1)\, \mathrm{e}^{-\mathrm{i}\left(Z\, \frac{\rho_1^2}{2} + \frac{\rho_1^4}{4}\right)}\, \mathrm{d}\rho_1 \\ &= \frac{1}{2\, \pi} \int_{-\infty}^\infty \int_{-\infty}^\infty \mathrm{e}^{-\mathrm{i}\left(R\, x_1 + Z\, \frac{x_1^2 + y_1^2}{2} + \frac{(x_1^2 + y_1^2)^2}{4}\right)}\, \mathrm{d}x_1 \mathrm{d}y_1. \qquad (2) \end{aligned}$$

Its square is shown in figure 1. In the Cartesian representation $x_1 = \rho_1 \cos\varphi$ and $y_1 = \rho_1 \sin\varphi$ are dimensionless coordinates in the plane of integration.

Expression (2) is the axially symmetric generalization of the Pearcey integral [7] $I_P(X,Z) = (2\,\pi)^{-1/2} \int_{-\infty}^{\infty} \exp\left[-\mathrm{i}\left(X\,x_1 + Z\,x_1^2/2 + x_1^4/4\right)\right] \mathrm{d}x_1$, which is also shown in figure 1.

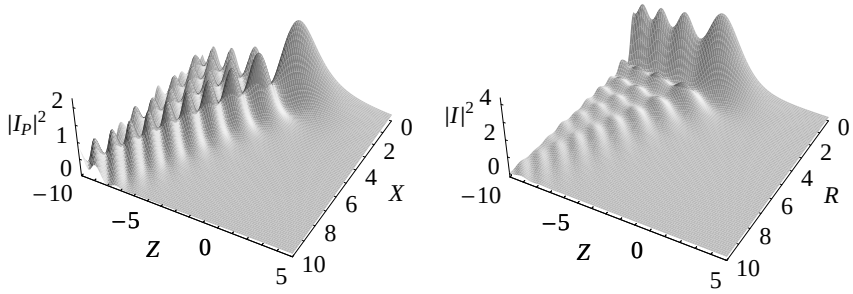

Figure 1. Absolute square of the Pearcey integral I_P (left) and the Bessoid integral I (right). The latter is proportional to the field of a spherically aberrated wave within small angles approximation

Both integrals correspond to so-called diffraction catastrophes [6]. Their field distribution contains caustic zones where the intensity predicted by geometrical optics goes to infinity. The Pearcey integral corresponds to a cusp caustic, i.e., a single one-dimensional curve in a two-dimensional space, and does not reveal a high intensity along the axis, while the Bessoid integral corresponds to a cuspoid caustic, i.e., to a surface of revolution of the cusp in three dimensions, as well as the caustic line up to the focus F at $z = Z = 0$. The equation of the cusp[a] is given by the semicubic parabola $27\,R^2 + 4\,Z^3 = 0$.

The cusp is the envelope of the family of rays. They correspond to the points of stationary phase in the Bessoid integral, i.e., those points where the two first partial derivatives with respect to R and Z of the phase

$$\phi \equiv -R\,x_1 - Z\,\frac{x_1^2 + y_1^2}{2} - \frac{(x_1^2 + y_1^2)^2}{4} \tag{3}$$

in the exponent in (2) vanish. Inside the cusp, for $27\,R^2 + 4\,Z^3 < 0$, three rays (tangents to the cusp) arrive at each point of observation $P \equiv (\rho, z)$, and outside, for $27\,R^2 + 4\,Z^3 > 0$, there is only one real ray (figure 2). Thus, the cusp forms the border between the lit region and the (partial) geometrical shadow.

[a] Normally, the term cusp refers to its vertex only, but we use it to denote the two branches. Besides, henceforth we will apply the term cusp also for the cuspoid.

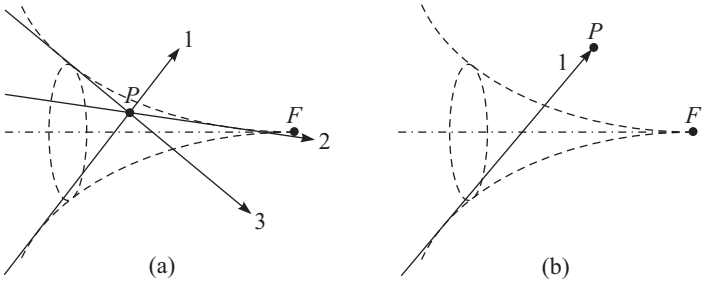

Figure 2. (a) 3-ray region inside the cuspoid (dashed line). (b) 1-ray region outside. The z-axis is represented by a dashed-dotted line

Without loss of generality, we assume that all rays lie in the meridional plane $\varphi = 0$ ($y_1 = 0$) and hence correspond to the roots $x_{1,j}$ ($j = 1, 2, 3$) of the cubic equation

$$R + Z\,x_1 + x_1^3 = 0\,, \tag{4}$$

which are given by Cardan's formulas [10]. On the axis, $R = 0$, a cone of an infinite number of rays converges. These rays originate from the circle $x_1^2 + y_1^2 = -Z$ on the aperture. They are all in phase and produce a high intensity along the axis (compare the two pictures in figure 1). The oscillations occur due to interference with the ray propagating along the z-axis.

2.2. *Asymptotic Expressions*

Off the caustic — away from the cusp and the focal line — the Bessoid integral can be approximated by the method of stationary phase [11]:

$$I(R, Z) \approx \sum_{j=1}^{m} \frac{\mathrm{e}^{\,\mathrm{i}\,\phi_j \,+\, \mathrm{i}\,\frac{\pi}{4}\,\operatorname{sign}\mathbf{H}_j}}{\sqrt{|\det \mathbf{H}_j|}}\,, \tag{5}$$

where the summation runs over all real rays, i.e., $m = 1$ (lit) or 3 (shadow). ϕ_j is obtained by inserting the j-th stationary point ($x_{1,j}, y_{1,j} = 0$) into the phase (3). The determinant and signature of the Hessian are given by

$$\det \mathbf{H}_j = Z^2 + 4\,x_{1,j}^2\,Z + 3\,x_{1,j}^4\,, \tag{6}$$

$$\operatorname{sign}\mathbf{H}_j = \operatorname{sgn}(-Z - 3\,x_{1,j}^2) + \operatorname{sgn}(-Z - x_{1,j}^2)\,. \tag{7}$$

Near the cusp the Bessoid integral shows an Airy-type behavior typical for caustics where two real rays disappear and become complex.

Near the axis (small R) one can derive the approximation

$$I(R,Z) \approx \frac{\sqrt{\pi}}{2}\, J_0(R\sqrt{-Z})\, \mathrm{e}^{\,\mathrm{i}\,\frac{Z^2-\pi}{4}}\ \mathrm{erfc}\!\left(\frac{Z}{2}\,\mathrm{e}^{\,\mathrm{i}\,\frac{\pi}{4}}\right), \tag{8}$$

where erfc is the complementary error function,[b] which can also be written in terms of Fresnel sine and cosine functions [9]. Expression (8) becomes exact for $R = 0$, where $J_0(0) = 1$. It shows that near the axis the Bessoid integral is virtually a Bessel-beam with a variable cross section.

2.3. *Numerical Evaluation*

As the Bessoid integrand is highly oscillatory, its evaluation for the whole range of coordinates R and Z is non-trivial and of large practical importance. Direct numerical integration along the real axis and the method of steepest descent in the complex plane both have their disadvantages. By far the fastest technique is based on the numerical solution of the *ordinary* differential equation [12]

$$L_R - Z\, I_R + \mathrm{i}\, R\, I = 0\,. \tag{9}$$

Indices denote (partial) derivatives and $L \equiv I_{RR} + I_R/R$ is an abbreviation for the radial Laplacian applied onto I. The three initial conditions at $R = 0$ are (i) $I(0,Z)$ calculated from (8), (ii) $I_R(0,Z) = 0$ due to symmetry and (iii) $L(0,Z) = Z\, I(0,Z) + \mathrm{i}$, arising from the fact that the Bessoid integral satisfies the paraxial Helmholtz equation $2\,\mathrm{i}\, I_Z + L = 0$.

In the literature the Pearcey integral was calculated by solving differential equations [13], by a series representation [14] and by the first terms of its asymptotic expansion [15]. The Bessoid integral was expressed in terms of parabolic cylinder functions [16] and as a series [9]. The latter work gives reference to an unpublished work of Pearcey [17], stating that differential equations for the Bessoid integral were employed there. No other indication of the existence of such equations is known to us.

2.4. *Geometrical Optics for the Cuspoid*

In geometrical optics, rays carry the information of amplitude and phase. The total field in a point P is given by the sum of all ray fields there. A ray's field at P is determined by

$$U(P) = U_0\, \frac{\mathrm{e}^{\,\mathrm{i}\,k\,\psi}}{\sqrt{J}}\,, \tag{10}$$

[b] http://mathworld.wolfram.com/Erfc.html

where U_0 is the amplitude at some initial wavefront, ψ is the eikonal (optical path along the ray from this wavefront to P) and J is the generalized geometrical divergence, which can be calculated from flux conservation along the ray [18]. For a homogeneous medium with constant refractive index $J = R_m R_s/(R_{m0} R_{s0})$, where R_m, R_s are the main radii of curvature at the point P and R_{m0}, R_{s0} on the initial wavefront, where $U = U_0$. Caustics correspond to an intersection of infinitesimally close rays ($R_m R_s \to 0$, $|U| \to \infty$). They are the envelopes of ray families and the rays are tangent to the caustic. When one crosses the caustic, an even number of rays appears or disappears.

When a ray touches the caustic, its radius of curvature changes the sign and the ray undergoes a phase delay of $-\pi/2$, which is taken into account by the proper choice of the square root in (10). When a ray touches several caustics, these delays must be added. The total caustic phase shift, denoted as $\Delta\varphi$, can be explicitly written in the phase. For the cuspoid topology and ray numbering ($j = 1, 2, 3$) according to figure 2, we obtain:

$$U(P) = U_0 \frac{\mathrm{e}^{\,\mathrm{i}\,k\,\psi}}{\sqrt{J}} = U_0 \frac{\mathrm{e}^{\,\mathrm{i}\,k\,\psi\,+\,\mathrm{i}\,\Delta\varphi}}{\sqrt{|J|}} \quad \text{with} \quad \Delta\varphi_j = \begin{cases} -\pi & \text{for } j = 1, \\ 0 & \text{for } j = 2, \\ -\pi/2 & \text{for } j = 3. \end{cases} \tag{11}$$

Ray 1 touched the cuspoid and the focal line, ray 2 is not shifted, and ray 3 touched the cuspoid.

3. Relation between Geometrical and Wave Optics

3.1. *Matching with the Bessoid Integral*

If we have found the phases $\varphi \equiv k\,\psi$ and divergences J of the rays, the (scalar) geometrical optics solution with an axially symmetric 3-ray cuspoid topology can be written as

$$U(\mathbf{r}) = \sum_{j=1}^{3} \frac{U_{0,j}\ \mathrm{e}^{\,\mathrm{i}\,\varphi_j(\mathbf{r})}}{\sqrt{J_j(\mathbf{r})}}\,. \tag{12}$$

Here $\mathbf{r} \equiv (\rho, z)$ are the real-space coordinates and we have allowed for different initial amplitudes $U_{0,j}$ of the rays. This field shows singularities at the caustic, especially on the axis, which is the most interesting region for applications. On the other hand, the paraxial spherically aberrated wave resulted in the Bessoid integral (2) which has no singularities.

We want to describe arbitrary axially symmetric focusing by matching the solution of geometrical optics (where it is correct) with a wave field

constructed from the Bessoid integral and its partial derivatives I_R and I_Z (*method of uniform caustic asymptotics*). We make the Ansatz [6]

$$U(\mathbf{r}) = \left(A(\mathbf{r})\, I(\mathbf{R}) + \frac{1}{\mathrm{i}}\, A_R(\mathbf{r})\, I_R(\mathbf{R}) + \frac{1}{\mathrm{i}}\, A_Z(\mathbf{r})\, I_Z(\mathbf{R}) \right) \mathrm{e}^{\,\mathrm{i}\,\chi(\mathbf{r})}\,. \qquad (13)$$

Here $\mathbf{R} \equiv (R, Z)$ are the yet unknown coordinates of the Bessoid integral, A, A_R and A_Z are three amplitude factors[c] and χ is a phase function. Now the stationary phase approximation of (13) is matched with the geometrical optics solution (12) by equating the amplitudes and phases:

$$\left(A(\mathbf{r}) + A_R(\mathbf{r})\, \phi_R(\mathbf{R}, \mathbf{t}_j) + A_Z(\mathbf{r})\, \phi_Z(\mathbf{R}, \mathbf{t}_j)\right) \frac{1}{\sqrt{H_j}} = \frac{U_{0,j}}{\sqrt{J_j}}\,, \qquad (14)$$

$$\chi(\mathbf{r}) + \phi(\mathbf{R}, \mathbf{t}_j) = \varphi_j(\mathbf{r})\,, \qquad (15)$$

where ϕ_R and ϕ_Z are the partial derivatives of (3) and $1/\sqrt{H_j} \equiv \mathrm{e}^{\,\mathrm{i}\,\frac{\pi}{4}\,\mathrm{sign}\,\mathbf{H}_j} / \sqrt{|\det \mathbf{H}_j|}$.[d]

The points of stationary phase were denoted as $\mathbf{t}_j \equiv (t_j, 0)$, where the t_j are given by Cardan's solutions of $R + Z\,t + t^3 = 0$. Note that stationary points[e] $\mathbf{t}_j = \mathbf{t}_j(\mathbf{R})$ and coordinates $\mathbf{R} = \mathbf{R}(\mathbf{r})$. The conditions (14) and (15) give 6 equations for the 6 unknowns R, Z, χ, A, A_R, and A_Z.

It is convenient to solve (15) using quantities that are permutationally invariant with respect to the roots t_j [8, 19]. This yields

$$\begin{aligned} R &= \sqrt{\frac{Z^3}{54} - \frac{4\,b_2}{9\,Z}}\,, \\ Z &= \pm \sqrt[4]{\frac{2}{3}} \sqrt{-2\,\mathrm{sgn}(b_3)\,\sqrt{b_2 + q} + 2\,\sqrt{2\,b_2 - q + 2\sqrt{b_2^2 - b_2\,q + q^2}}}\,, \\ \chi &= b_1 - \frac{1}{6}\,Z^2\,, \end{aligned} \qquad (16)$$

where $\mathrm{sgn}(Z) = \mathrm{sgn}(Z^4 - 24\,b_2)$. The b_l $(l = 1, 2, 3)$ are given by $b_1 \equiv (1/3)\sum_{j=1}^{3} \varphi_j$, $b_2 \equiv \sum_{j=1}^{3} (\varphi_j - b_1)^2$ and $b_3 \equiv \sum_{j=1}^{3} (\varphi_j - b_1)^3$. The quantity q can be expressed in different ways:

$$\begin{aligned} q^3 \equiv 6\,b_3^2 - b_2^3 &= \frac{1}{2^{11}}\,R^2\,(27\,R^2 + 4\,Z^3)^3 \\ &= -2\,(\varphi_1 - \varphi_2)^2\,(\varphi_2 - \varphi_3)^2\,(\varphi_3 - \varphi_1)^2\,. \end{aligned} \qquad (17)$$

[c] The indices R and Z in the amplitude factors do not indicate derivatives.
[d] Outside the cusp, the rays 2 and 3 are complex and the definition of H_j is more subtle.
[e] The partial derivatives with respect to R and Z in (14) must be evaluated in such a way as the t_j were held constant, although they are functions of $\mathbf{R}$ themselves.

Hence, it vanishes exactly at the caustic where two phases are equal.[f]

The solutions of (14) are

$$\begin{aligned} A &= -\,U_{0,1}\,\frac{\sqrt{H_1}}{\sqrt{J_1}}\,\frac{t_2\,t_3}{(t_3-t_1)\,(t_1-t_2)} - \ldots - \ldots \text{ (cyclic)}\,, \\ A_R &= U_{0,1}\,\frac{\sqrt{H_1}}{\sqrt{J_1}}\,\frac{t_1}{(t_3-t_1)\,(t_1-t_2)} + \ldots + \ldots \text{ (cyclic)}\,, \\ A_Z &= 2\,U_{0,1}\,\frac{\sqrt{H_1}}{\sqrt{J_1}}\,\frac{1}{(t_3-t_1)\,(t_1-t_2)} + \ldots + \ldots \text{ (cyclic)}\,, \end{aligned} \tag{18}$$

where the cyclic terms permutate the numbering of rays: $(1,2,3) \rightarrow (2,3,1) \rightarrow (3,1,2)$. The Bessoid matching solution (13) does not show the divergences of geometrical optics.

3.2. *General Expressions On and Near the Axis*

Inside the cusp ($z < f$), the formulas can be strongly simplified on and near the axis (small ρ). From figure 3 one can see that up to the first order in ρ the phases can be written as

$$\varphi_1 = \varphi_{\rm np} + k\,\rho\,\sin\beta\,, \quad \varphi_2 = \varphi_{\rm p}\,, \quad \varphi_3 = \varphi_{\rm np} - k\,\rho\,\sin\beta\,. \tag{19}$$

Here $\varphi_{\rm np}$ and $\varphi_{\rm p}$ denote the phases of the non-paraxial rays and the (par)axial ray (with $\rho = 0$).

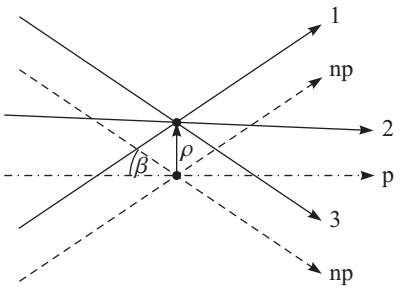

Figure 3. Near the axis, the phases of the rays 1 and 3 differ from the phase of the non-paraxial rays by $\pm\,k\,\rho\,\sin\beta$, whereas the phases of ray 2 and the (par)axial ray are the same in first order. The non-paraxial ray crosses the axis at the angle $\beta > 0$

We insert these phases into the exact expressions in (16), Taylor expand with respect to ρ and resubstitute $\varphi_{\rm np} = (\varphi_1 + \varphi_3)/2$, $\varphi_{\rm p} = \varphi_2$ and

[f] At the cuspoid $\varphi_2 = \varphi_3$ $(27\,R^2 + 4\,Z^3 = 0)$ and on the axis $\varphi_1 = \varphi_3$ $(R = 0)$.

$k\,\rho\,\sin\beta = (\varphi_1 - \varphi_3)/2$ from (19). This yields

$$R = \frac{(\varphi_1 - \varphi_3)/2}{\sqrt{2}\,\sqrt[4]{(\varphi_1 + \varphi_3)/2 - \varphi_2}} = \frac{k\,\rho\,\sin\beta}{\sqrt{-Z}}\,, \tag{20}$$

$$Z = -2\sqrt{\frac{\varphi_1 + \varphi_3}{2} - \varphi_2} = -2\,\sqrt{\varphi_{\mathrm{np}} - \varphi_{\mathrm{p}}}\,. \tag{21}$$

On the axis $\rho = 0$, we obtain $R = 0$ and $Z = -2\,\sqrt{\varphi_1 - \varphi_2}$. The Bessoid integral has its global maximum at $Z_{\mathrm{m}} \approx -3.051$. This corresponds to the phase difference

$$\varphi_1 - \varphi_2 = Z_{\mathrm{m}}^2/4 \approx 2.327\,. \tag{22}$$

The geometrical meaning of this result is that ray 1 and 3 are shifted by $-\pi/2$ as they touch the cusp. In addition, they acquire a further shift of $-\pi/2$ when crossing the focal line. But exactly *on the axis* only half of this delay has occurred yet, which yields $\varphi_1 - \varphi_2 \approx 3\,\pi/4 \approx 2.356$, which is close to 2.327. This is the condition for the (first) constructive interference of the axial and the non-paraxial rays.

The width of the focal line caustic, ρ_w, is defined by the first zero $w_0 \approx 2.405$ of the Bessel function in (8). Hence, with (20),

$$\rho_w \equiv \frac{w_0}{k\sin\beta} \approx 0.383\,\frac{\lambda}{\sin\beta}\,. \tag{23}$$

In the geometrical optics picture the first minimum occurs when ray 1 and 3 interfere destructively, i.e., when their phase difference becomes π. This results in $\varphi_1 - \varphi_3 = \pi + \pi/2$, where the term $\pi/2$ takes into account the caustic phase shift of ray 1: $\rho_w \approx (\varphi_1 - \varphi_3)/2\,k\sin\beta = 0.375\,\lambda/\sin\beta$.

Finally, we present an expression for the field (13) on the axis. The equations for the amplitudes (18) simplify tremendously. Furthermore, we use the linear relationship between the Bessoid and its Z-derivative, $\mathrm{i}\,Z\,I(0,Z) - 2\,I_Z(0,Z) = 1$. Finally, we end up with [12]

$$U = \left[\frac{U_{0,1}\,\sqrt{2\,k\,\rho\,\sin\beta}}{\sqrt{J_1}}\left(\mathrm{i}\,I - \frac{1}{Z}\right) + \frac{U_{0,2}}{\sqrt{J_2}}\right]\mathrm{e}^{\,\mathrm{i}\,\varphi_2}\,. \tag{24}$$

Note that (inside the cusp) on the axis ($\rho \to 0$) both $1/\sqrt{J_2}$ and the ratio $\sqrt{\rho}/\sqrt{J_1}$ remain finite.

3.3. *Angular Dependences and Vectorial Problems: Higher-order Bessoid Matching*

Often — especially in vectorial problems (see section 4) — there exists axial symmetry with respect to the wavefronts, ray phases and generalized

divergences, but not with respect to the amplitudes. In this case, new functions are required to represent arbitrary angular dependence of the field. The natural generalization of (2) are the *higher-order Bessoid integrals* [16] with the non-negative integer m:

$$I_m(R,Z) = \int_0^\infty \rho_1^{m+1}\, J_m(R\,\rho_1)\, \mathrm{e}^{-\mathrm{i}\left(Z\,\frac{\rho_1^2}{2}+\frac{\rho_1^4}{4}\right)}\,\mathrm{d}\rho_1, \tag{25}$$

where $I_0 \equiv I$. They obey the recurrence relation [12] $I_{m+1} = -I_{m,R} + m\,I_m/R$. The integral I_m is canonical for angular dependent geometrical field components $U^{(m)}(\rho,z)\,\sin m\,\varphi$ or $U^{(m)}(\rho,z)\,\cos m\,\varphi$. In matching similar to (13), the angular dependence cancels. Since higher-order Bessoid integrals can be written in terms of I_0, it can be shown that the points of stationary phase, the matching of phases and thus the higher-order coordinates and phases are identical with the original ones. From the physical point of view, this reflects the conservation of the wavefront and thus the ray phases and divergences.

The equations for the amplitudes have to be generalized. The higher-order amplitudes A_m, A_{mR} and A_{mZ} have the same form as (18) but with an additional factor $(\mathrm{i}\,t_j)^m$ in each denominator [12], e.g.,

$$A_m = -U_{0,1}\,\frac{\sqrt{H_1}}{\sqrt{J_1}}\,\frac{t_2\,t_3}{(\mathrm{i}\,t_1)^m\,(t_3-t_1)\,(t_1-t_2)} - \ldots - \ldots \text{ (cyclic)}\,. \tag{26}$$

4. The Sphere

4.1. *Geometrical Optics Solution*

Consider a plane wave falling on a transparent sphere in vacuum. Figure 4 illustrates the refraction of a single ray in the meridional plane, containing the point of observation P and the axis. Within the frame of geometrical optics the cuspoid is formed behind the sphere in analogy to figure 2.

Let a be the sphere radius and $n > 1$ its refractive index. The center M is located at the origin of an axially symmetric cylindrical coordinate system (ρ, z). The incident plane wave propagates parallel to the z-axis. The geometrical optics focus, formed by the paraxial rays, is located at $F \equiv (0, f)$ with $f \equiv a\,n/[2\,(n-1)]$ [20].

A ray passes the point Q, is first refracted at Q_1, a second time at Q_2 and propagates to P. The incident and transmitted angle, θ_i and θ_t, are related by Snell's law, $\sin\theta_i = n\sin\theta_t$. Writing the position of $P \equiv (\rho, z)$ in polar coordinates, $\rho = l\sin\theta$ and $z = l\cos\theta$, one can find the following

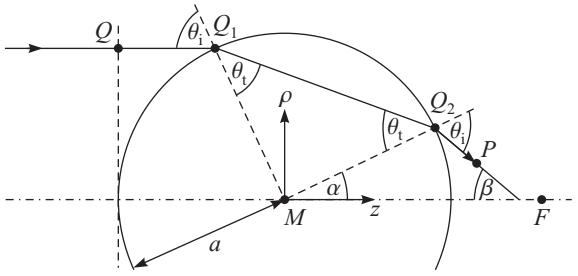

Figure 4. Refraction of a ray — propagating from Q to P — by a sphere with radius a and refractive index n. The picture is drawn in the meridional plane and all indicated angles are positive

expression, determining the three rays that arrive at P:

$$l \sin(\theta + 2\,\theta_i - 2\,\theta_t) = a \sin\theta_i, \tag{27}$$

where one has to substitute $\theta_t = \arcsin[(\sin\theta_i)/n]$. This is a transcendental cubic-like equation which has three roots,[g] either all real or one real and two complex conjugate. We denote them as $\theta_{i,j}$ $(j = 1, 2, 3)$ and choose their order consistently with the previous notations.[h] When the $\theta_{i,j}$ are known, we find the $\theta_{t,j}$ from Snell's law and the α_j and β_j from $\alpha_j = 2\,\theta_{t,j} - \theta_{i,j}$ and $\beta_j = 2\,\theta_{i,j} - 2\,\theta_{t,j}$. Omitting the index j, the three ray coordinates can be written as $s \equiv \overline{Q_2P} = (l\cos\theta - a\cos\alpha)/\cos\beta$. The eikonal is the optical path accumulated from Q to P (on the dashed vertical line in figure 4 all rays are still in phase):

$$\psi = \overline{QQ_1} + n\,\overline{Q_1Q_2} + \overline{Q_2P} - a = a\,(2\,n\cos\theta_t - \cos\theta_i) + s\,. \tag{28}$$

We have subtracted the sphere radius a from the path contributions to make the eikonal zero in the center M, if there were no sphere.

Next we calculate the geometrical optics amplitudes by determining the meridional and sagittal radii of curvature, R_m and R_s, and their changes due to refraction. Formulas for the refraction on an arbitrary surface with arbitrary orientation of the main radii are given in Refs. [18, 21]. A simple derivation for the sphere can be found in Ref. [12]. It yields the dependence of the actual radii of curvature R_m and R_s (right after the refraction) on

[g] For $n \geq \sqrt{2}$ this is true for $z \geq a$. If $n < \sqrt{2}$, the 3-ray region does not start until some distance behind the sphere.

[h] Therefore, $\theta_{i,1}$ is always real and negative, whereas $\theta_{i,2}$ and $\theta_{i,3}$ are either real and positive (lit region) with $\theta_{i,2} < \theta_{i,3}$ or complex conjugate (geometrical shadow).

the initial radii R_{m0} and R_{s0} (just before the refraction):

$$R_m = \frac{n\,a\,R_{m0}\cos^2\theta_t}{a\cos^2\theta_i + R_{m0}\,(\cos\theta_i - n\cos\theta_t)},\ R_s = \frac{n\,a\,R_{s0}}{a + R_{s0}\,(\cos\theta_i - n\cos\theta_t)}. \tag{29}$$

For a plane wave, $R_{m0}, R_{s0} \to \infty$, the radii of curvature in the points Q_1 (inside the sphere) and Q_2 (outside the sphere) have the compact form

$$\begin{aligned} R_{m,Q_1} &= -a\,\frac{\sin\theta_i\cos^2\theta_t}{\sin(\theta_i-\theta_t)}\,, \quad R_{m,Q_2} = -a\,\frac{\cos\theta_i}{2}\left(\frac{\cos\theta_i\sin\theta_t}{\sin(\theta_i-\theta_t)} - 1\right), \\ R_{s,Q_1} &= -a\,\frac{\sin\theta_i}{\sin(\theta_i-\theta_t)}\,, \qquad R_{s,Q_2} = -a\,\frac{\sin(2\,\theta_t-\theta_i)}{\sin(2\,\theta_i-2\,\theta_t)}\,. \end{aligned} \tag{30}$$

The overall geometrical generalized divergence after both refractions reads (index j omitted)

$$\frac{1}{\sqrt{J}} = \frac{\sqrt{R_{m,Q_1}\,R_{s,Q_1}}}{\sqrt{(R_{m,Q_1}+d)\,(R_{s,Q_1}+d)}}\,\frac{\sqrt{R_{m,Q_2}\,R_{s,Q_2}}}{\sqrt{(R_{m,Q_2}+s)\,(R_{s,Q_2}+s)}}\,, \tag{31}$$

where $d \equiv 2\,a\cos\theta_t$ is the distance of propagation within the sphere. Note that ray 1 has a negative angle θ_i. Besides, double caustic phase shift should be inserted manually for this ray (minus sign) as in (11). The caustic shifts of the rays 2 and 3 are taken into account automatically by the standard definition of the square root.

Finally, the geometrical optics solution for the sphere is given by (12),[i] where the eikonal ψ and divergence J are given by (28) and (31). The equation determining the three rays is (27).

To incorporate Fresnel transmission coefficients, we assume that the incident light is linearly polarized in x-direction, i.e., the incident electric field vector is $\mathbf{E}_0 = E_0\,\mathbf{e}_x$, with $\mathbf{e}_x$ the unit vector in x-direction and $E_0 \equiv U_0$. Since axial symmetry is broken, we introduce the polar angle φ which is measured from x to y. The point of observation $P \equiv (\rho, \varphi, z)$ will be reached by three rays (two may be complex) and their angles $\theta_{i,j}$ are still determined by (27), for all three rays lie in the meridional plane, containing P and the z-axis (figure 5a).

The initial π- and σ-polarized components depend on φ: $E_{0,\pi} = E_0\cos\varphi$ and $E_{0,\sigma} = E_0\sin\varphi$ (figure 5b). We define the overall transmission coefficients $T_\pi \equiv t_{12,\pi}\,t_{21,\pi} = 1 - r_{12,\pi}^2$, and $T_\sigma \equiv t_{12,\sigma}\,t_{21,\sigma} = 1 - r_{12,\sigma}^2$. Here the t_{12} (r_{12}) are the standard Fresnel transmission (reflection) coefficients [5] from the medium 1, i.e., vacuum, into the medium 2, i.e., the sphere.

[i] In the geometrical shadow the sum becomes only the term with $j = 1$.

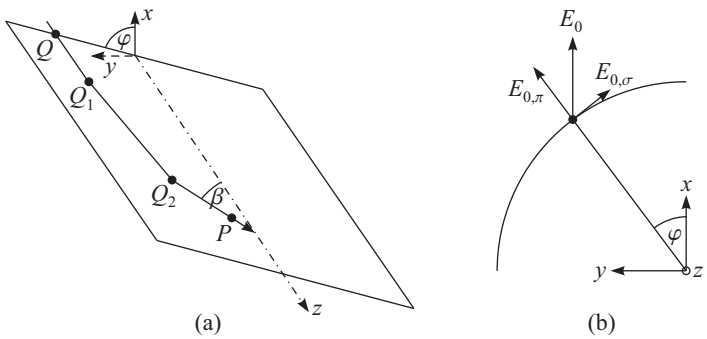

Figure 5. (a) A ray propagates from Q to P in the meridional plane (plane of incidence). (b) Decomposition of the initial electric field vector with length E_0 into its π- and σ-component parallel and perpendicular to the meridional plane

The ray field behind the sphere is found by the projection onto the original Cartesian system (x, y, z). We write the components of the transmission vector $\mathbf{T} \equiv (T_x, T_y, T_z)$ and show the ray index $j = 1, 2, 3$ explicitly. The φ-dependence is indicated with the superscript (m):

$$\begin{aligned} T_{x,j} &= T_j^{(0)} + T_j^{(2)} \cos 2\,\varphi\,, & T_j^{(0)} &\equiv \frac{T_{\pi,j} \cos\beta_j + T_{\sigma,j}}{2}\,, \\ T_{y,j} &= T_j^{(2)} \sin 2\,\varphi\,, \quad \text{where} & T_j^{(1)} &\equiv T_{\pi,j} \sin\beta_j\,, \\ T_{z,j} &= T_j^{(1)} \cos\varphi\,, & T_j^{(2)} &\equiv \frac{T_{\pi,j} \cos\beta_j - T_{\sigma,j}}{2}\,. \end{aligned} \tag{32}$$

Hence, the geometrical optics solution for the electric field $\mathbf{E} \equiv (E_x, E_y, E_z)$ — including the eikonal ψ (28) and divergence J (31) — reads

$$\begin{aligned} E_{x,j} &= E_j^{(0)} + E_j^{(2)} \cos 2\,\varphi\,, \\ E_{y,j} &= E_j^{(2)} \sin 2\,\varphi\,, \quad \text{where} \quad E_j^{(m)} \equiv E_0\, \frac{T_j^{(m)}\, \mathrm{e}^{\,\mathrm{i}\,k\,\psi_j}}{\sqrt{J_j}}\,. \\ E_{z,j} &= E_j^{(1)} \cos\varphi\,, \end{aligned} \tag{33}$$

4.2. *The Bessoid Matching Solution*

Matching each term $E^{(m)} = \sum_{j=1}^{3} E_j^{(m)}$ by the Ansatz (13) in its higher-order formulation with the corresponding integral I_m, we obtain the vectorial electric field in the form

$$\mathbf{E}(\rho, \varphi, z) = \begin{pmatrix} E_x \\ E_y \\ E_z \end{pmatrix} = E^{(0)} \begin{pmatrix} 1 \\ 0 \\ 0 \end{pmatrix} + E^{(1)} \begin{pmatrix} 0 \\ 0 \\ \cos\varphi \end{pmatrix} + E^{(2)} \begin{pmatrix} \cos 2\,\varphi \\ \sin 2\,\varphi \\ 0 \end{pmatrix}. \tag{34}$$

Figure 6 illustrates the intensity, i.e., the absolute square of the electric field $|E|^2 \equiv \mathbf{E}\,\mathbf{E}^*$, for $\varphi = 0$ (x,z-plane) and $\varphi = \pi/2$ (y,z-plane).

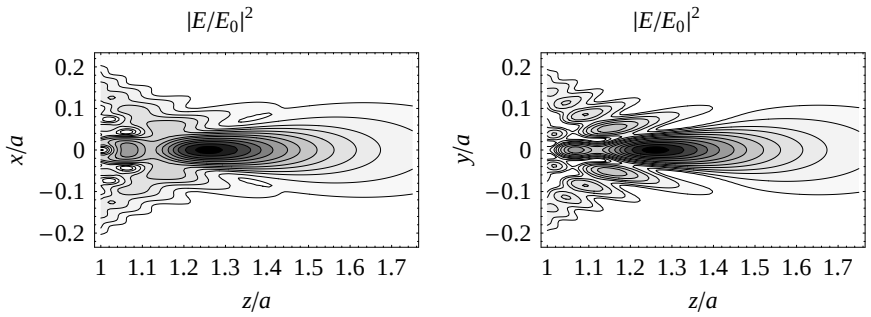

Figure 6. Normalized intensity $|E/E_0|^2$ in the normalized x,z-plane (left) and in the y,z-plane (right). Contour shadings go from white (zero) to black (≈ 700). Parameters: refractive index $n = 1.5$, dimensionless wavenumber $k\,a = 100$. The initial electric field amplitude is $\mathbf{E}_0 = E_0\,\mathbf{e}_x$. The sphere with radius a is situated in the origin. The focus of geometrical optics is located at $z = f = 1.5\,a$, whereas the diffraction focus — the point of maximum intensity — is significantly shifted towards the sphere: $f_d \approx 1.25\,a$. In dimensional units, for a wavelength of $\lambda = 0.248\,\mu$m the sphere radius is $a \approx 4\,\mu$m

The magnetic field $\mathbf{H}$ can be calculated similarly (incident magnetic field $\mathbf{H}_0 = H_0\,\mathbf{e}_y$, $H_0 = E_0$) and the (normalized) Poynting vector is given by $\mathbf{S} \equiv \mathrm{Re}(\mathbf{E}\times\mathbf{H}^*)$.

4.3. *On the Axis*

On the axis the electric field is given by its x-component only (direction of polarization) due to averaging over φ in (34). For $z < f$ (inside the cusp) it is given by the analytical expression (24). After several simplifications [12] it can be written as

$$E = E_0 \left[T_1\, D_1 \left(\mathrm{i}\, I - \frac{1}{Z} \right) + \frac{T_2}{1 - z/f} \right] \mathrm{e}^{\,\mathrm{i}\,\varphi_2} \tag{35}$$

where the transmission factors $T_j \equiv T_j^{(0)}$ are given in (32) and for dielectric spheres have the form:

$$T_1 = \frac{n\,(1 + 3\cos\beta_1)\cos\theta_{i,1}\cos\theta_{t,1}}{(n\cos\theta_{i,1} + \cos\theta_{t,1})^2}, \quad T_2 = \frac{4\,n}{1 + n^2}. \tag{36}$$

The phases in the coordinate $Z = -2\sqrt{\varphi_1 - \varphi_2}$ are given by

$$\varphi_1 = \varphi_3 = k\,a\left(2\,n\cos\theta_{t,1} - \cos\theta_{i,1} + \frac{\sin\alpha_1}{\sin\beta_1}\right),\ \varphi_2 = k\,a\,(2\,n-2) + k\,z\,, \tag{37}$$

and $D_1 \equiv \sqrt{\varphi_1 - \varphi_3}/\sqrt{J_1}$ is the first ray's compensated divergence:[j]

$$\begin{aligned} D_1 &= -\frac{\sqrt{(R_{m,Q_1})_1\,(R_{s,Q_1})_1}}{\sqrt{[(R_{m,Q_1})_1 + d_1]\,[(R_{s,Q_1})_1 + d_1]}}\,\frac{\sqrt{(R_{m,Q_2})_1\,(R_{s,Q_2})_1}}{\sqrt{(R_{m,Q_2})_1 + s_1}}\,\sqrt{2\,k}\,\sin\beta, \\ &= -2\,\sqrt{2\,k\,a}\,\cos(\beta_1/2)\,\sqrt{\frac{\cot\theta_{i,1}\cos\theta_{t,1}\sin(\beta_1/2)}{1 + 1/n^2 - 3\sin^2(\beta_1/2)/\sin^2\theta_{i,1}}}. \end{aligned} \tag{38}$$

which manifestly has no singularity until the geometrical focus where $(R_{m,Q_2})_1 + s_1 \to 0$. Equation (35) is valid even near the focus, since the diverging terms D_1/Z and $(1 - z/f)^{-1}$ almost cancel. For $z \to f$, however, the divergence of D_1 itself becomes important, as the non-paraxial ray 1 becomes axial.

In figure 7 we show the position and the value of the maximum of $|E|^2$ as a function of the refractive index and the dimensionless product $k\,a$, calculated from (35). The z-coordinate of this global maximum is denoted with f_d (diffraction focus) and the intensity there is $|E(f_d)|^2$.

The main contribution in (35) stems from the Bessoid integral, that is from the term $\propto T_1\,D_1\,I$. Thus, the position of the maximum can be estimated from condition (22), i.e., $\varphi_1 - \varphi_2 \approx 3\,\pi/4$. If the phase difference $\varphi_1 - \varphi_2$ from (37) is expressed as a function of $\theta_{i,1}$, Taylor expanded and equated to $3\,\pi/4$, then we get in the lowest non-trivial order of the inverse product $k\,a$:[k]

$$f_d \approx \frac{a}{2}\,\frac{n}{n-1}\left(1 - \sqrt{\frac{3\,\pi}{4\,k\,a}\,\frac{n\,(3-n)-1}{n\,(n-1)}}\right). \tag{39}$$

[j] The minus sign on the right hand side comes from the manually inserted phase shift of the first ray. The structure of this equation (first line only) is general and is valid for arbitrary axially symmetric systems. D_1 is always finite on the axis, since both the sagittal radius of curvature and the phase difference $\varphi_1 - \varphi_3$ are proportional to the distance ρ.

[k] The factor $3\,\pi/4 \approx 2.356$ can be replaced by the more exact Bessoid value 2.327. Expression (39) approximates the position of the maximum within an error of about $< 5\,\%$ for $k\,a > 100$ and values of the refractive index near $1.4 < n < 1.6$. The transcendental phase difference condition itself, which holds for large angles, naturally has a wider range of applicability.

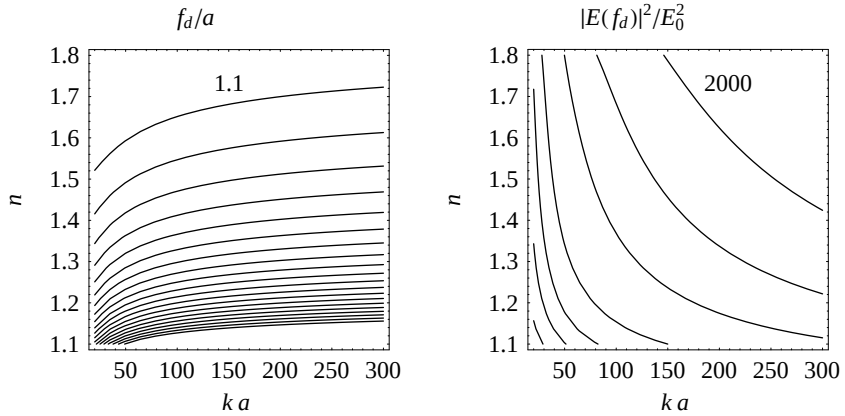

Figure 7. Left: Diffraction focus in units of the sphere radius as a function of n and $k\,a$ (contour lines from top to bottom go from 1.1 to 3.0 in steps of 0.1). Right: Intensity enhancement at f_d (contour lines from bottom left to top right are 20, 50, 100, 200, 500, 1000 and 2000)

Hence, in the limit of small wavelengths or large spheres the relative difference between the diffraction and the geometrical focus decreases proportionally to the inverse square root of $k\,a$.

4.4. *Comparison with the Theory of Mie*

We presented a general way to match geometrical optics solutions with the Bessoid integrals. It can be applied to any axially symmetric system with the cuspoid topology of spherical aberration.

For the sphere we can compare our approximate results with the theory of Mie [4]. A main quantity characterizing the sphere is the dimensionless Mie parameter $q \equiv k\,a$. Figure 8 compares the intensity on the axis obtained from the Mie theory with the Bessoid approximation. The parameters are as in figure 6 and the Mie parameter is $q = 300$, 100, 30 and 10.

We see very good agreement down to $q \approx 30$ ($a/\lambda \approx 4.8$). For $q = 10$ ($a/\lambda \approx 1.6$) the asymptotic behavior far from the sphere is still correct. However, for small q the characteristic scale a is no longer large compared to the wavelength λ and geometrical optics becomes invalid.

Next, we compare the off-axis electric and magnetic field as well as the z-component of the Poynting vector, S_z. Right behind the sphere ($z = a$) the agreement is not perfect (see again figure 8), most probably due to evanescent contributions, which are taken into account in the Mie theory. If we assume that they disappear at a distance of about $\lambda/2$ from the

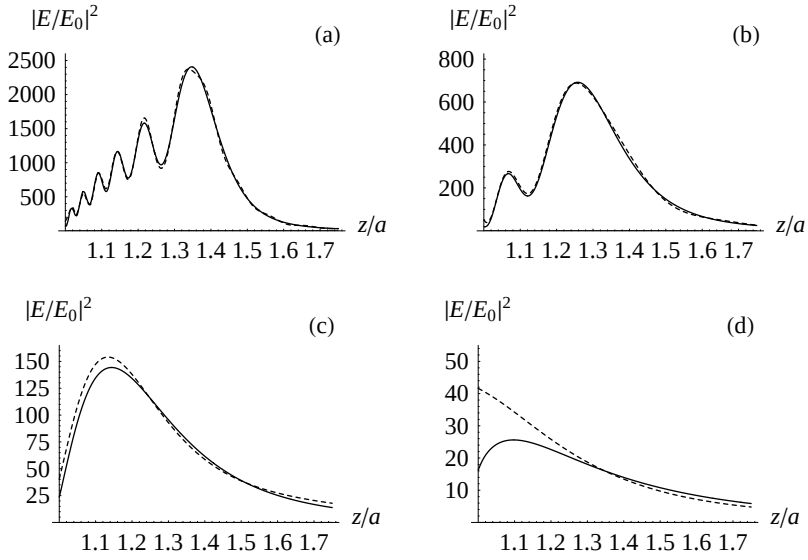

Figure 8. $|E/E_0|^2$ on the axis. Dashed lines represent the Mie theory, solid lines are the results of Bessoid matching. The cases (a), (b), (c) and (d) correspond to $q = 300$, 100, 30 and 10, respectively. In dimensional units, for $\lambda = 0.248\,\mu$m this corresponds to sphere radii of $a \approx 12\,\mu$m, $4\,\mu$m, $1.2\,\mu$m and $0.4\,\mu$m

sphere surface, good correspondence is expected for distances $z \geq a + \lambda/2$, i.e., $z/a \geq 1 + \pi/q$. For $q = 100$ this results in $z/a \gtrsim 1.03$. The following sections are made at $z = 1.02\,a$, showing good agreement (figure 9). For $z \gtrsim 1.05\,a$ the pictures become indistinguishable and even at $z = a$ all qualitative features are preserved.

The double-peak structure of $|E|^2$ along the direction of polarization has a purely geometrical origin. It is mainly related to the axial field component and is unrelated to near field effects. This is explained in detail in Ref. [12], where the estimation for the distance of the maxima from the axis is also given.

5. Conclusions

We described theoretically general axially symmetric aberrated focusing and studied light focusing by microspheres as an example. Following the method of uniform caustic asymptotics in Ref. [6], we introduced a canonical integral describing the field for the given cuspoid ray topology. This Bessoid integral appears naturally in the approximation of small angles. In some

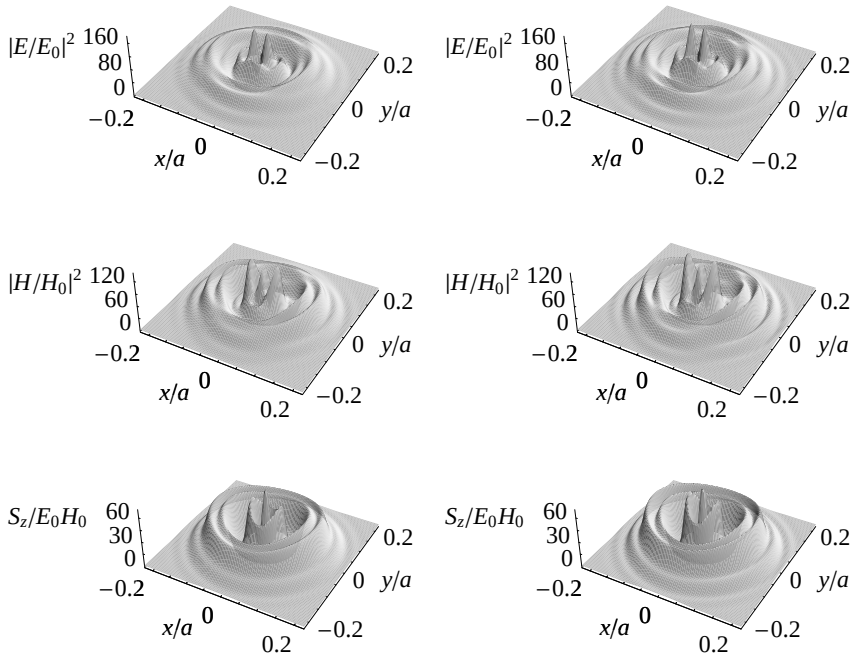

Figure 9. Normalized $|E|^2$, $|H|^2$ and S_z in the normalized x,y-plane for $z = 1.02\,a$ calculated with Bessoid matching (left) and with the Mie theory (right). The parameters are the same as in figure 6.

regions (off the caustic or exactly on the axis) it reduces to simple analytical expressions. In other regions we efficiently computed this highly oscillatory integral using a single ordinary differential equation.

For arbitrary axially symmetric and strongly spherically aberrated focusing, coordinate and amplitude transformations match the Bessoid wave field and the solution of geometrical optics. Caustic divergences of the latter are removed thereby. For vectorial problems with angular dependent field components, higher-order Bessoid integrals are used for the matching. The formulas significantly simplify on and near the axis. An approximate universal condition for the diffraction focus can be given in terms of phase differences. Here, the concept of caustic phase shifts is of main importance.

The central part of the Bessoid integral is essentially a Bessel beam with a variable cross section due to the variable angle of the non-paraxial rays. Its local diameter is always smaller than in the focus of an ideal lens with

the same numerical aperture. Besides, the largest possible apertures can be physically realized, which is hardly possible with lenses. All this is achieved at the expense of longitudinal confinement.

As an example the focusing of a linearly polarized plane wave by a transparent sphere is studied in detail. We calculate the geometrical optics eikonals and divergences, incorporate Fresnel transmission coefficients and perform Bessoid matching. Using the general theory, simple expressions for the light field on the axis and for the diffraction focus are derived. The two strong maxima in the intensity observed immediately behind the sphere can be explained as well.

Finally, the results of the Bessoid matching procedure are compared with the theory of Mie. The agreement is good for Mie parameters $k\,a > 30$. Near the sphere the correspondences is worse due to unaccounted evanescent contributions. With small radius to wavelength ratio geometrical optics breaks down and deviations increase everywhere.

The whole approach and the developed formulas can be applied in other areas of physics where axially symmetric focusing is of importance, e.g., acoustics, semiclassical quantum mechanics, radio wave propagation, scattering theory, etc.

Acknowledgments

The authors want to thank Prof. D. Bäuerle (Applied Physics, University of Linz) for stimulating discussions on microsphere patterning experiments, which initiated this study. The program used for the Mie calculations was provided by Prof. B. Luk'yanchuk and Dr. Z. B. Wang (both at the Data Storage Institute, Singapore). N. A. thanks Prof. V. Palamodov (Tel Aviv University) for illuminating mathematical suggestions, and the FWF (Austrian Science Fund) as well as the Christian Doppler Laboratory of Surface Optics (University of Linz) for financial support. We are indebted to Prof. D. Kane (Macquarie University Sydney) for the invitation to contribute to this book.

References

1. Luk'yanchuk, B. (Editor), *Laser Cleaning*, World Scientific Publishing (2002)
2. Bäuerle, D., *Laser Processing and Chemistry*, Springer–Verlag, 3rd Edition (2000)
3. Bäuerle, D., Landström, L., Kofler, J., Arnold, N., and Piglmayer, K., Laser-processing with colloid monolayers, Proc. SPIE **5339** (2004), 20–26

4. Mie, G., *Beiträge zur Optik trüber Medien, speziell kolloidaler Matallösungen*, Ann. d. Physik (4), **25** (1908), 377
5. Born, M. and Wolf, E., *Principles of Optics*, Cambridge University Press, 7^{th} Edition (2002)
6. Kravtsov, Y. A. and Orlov, Y. I., *Caustics, Catastrophes and Wave Fields*, Springer Series on Wave Phenomena (Vol. 15), Springer–Verlag, 2^{nd} Edition (1999)
7. Pearcey, T., *The structure of an electromagnetic field in the neighbourhood of a cusp of a caustic*, Lond. Edinb. Dubl. Phil. Mag. **37** (1946), 311–317
8. Connor, J. N. and Farrelly, D., *Theory of cusped rainbows in elastic scattering: uniform semiclassical calculations using Pearcey's Integral*, J. Chem. Phys. **75**(6) (1981), 2831–2846
9. Kirk, N. P., Connor, J. N., Curtis, P. R., and Hobbs, C. A., *Theory of axially symmetric cusped focusing: numerical evaluation of a Bessoid integral by an adaptive contour algorithm*, J. Phys. A: Math. Gen. **33** (2000), 4797–4808
10. Bronstein, I. N. and Semendjajew, K. A., *Handbook of Mathematics*, Springer–Verlag, 4^{th} Edition (2004)
11. Focke, J., W*ellenoptische Untersuchungen zum Öffnungsfehler*, Optica Acta **3** (1956), 110
12. Kofler, J., *Focusing of Light in Axially Symmetric Systems within the Wave Optics Approximation*, Master Thesis, University of Linz, Austria (2004)
13. Connor, J. N. and Curtis, P. R., *Differential equations for the cuspoid canonical integrals*, J. Math. Phys. **25**(10) (1984), 2895–2902
14. Connor, J. N., *Semiclassical theory of molecular collisions: Three nearly coincident classical trajectories*, Mol. Phys. **26** (1973), 1217–1231
15. Stamnes, J. J. and Spjelkavik, B., *Evaluation of the field near a cusp of a caustic*, Optica Acta **30** (1983), 1331–1358
16. Janssen, A. J., *On the asymptotics of some Pearcey-type integrals*, J. Phys. A: Math. Gen. **25** (1992), L823–L831
17. Pearcey, T. and Hill, G. W., *Spherical aberrations of second order: the effect of aberrations upon the optical focus*, Melbourne: Commonwealth Scientific and Industrial Research Organization (1963), 71–95
18. Kravtsov, Y. A. and Orlov, Y. I., *Geometrical Optics of Inhomogeneous Media*, Springer Series on Wave Phenomena (Vol. 6), Springer–Verlag (1990)
19. Brekhovskikh, L. M. and Godin, O. A., *Acoustics of Layered Media II*, Springer Series on Wave phenomena (Vol. 10), Springer–Verlag (1992)
20. Bergmann, L. and Schäfer, C., *Lehrbuch der Experimentalphysik* (Band 3), Optik (Hrsg: Gobrecht, H.), Walter de Gruyter, 7. Auflage (1978)
21. Červený, V., *Seismic Ray Theory*, Cambridge University Press (2001)